negative stages 2 and 3 and defective T-cell receptor gene expression due to unsuccessful recombination, which consequently causes apoptosis (Wakabayashi et al., 2003b; Ikawa et al., 2010; Li et al., 2010a,b). As designed for the detection of foreign molecules, the vomeronasal system shares similarities with the immune system. Both systems are responsible for self- vs non-self-recognition by expressing one receptor per cell from a large repertoire of receptor genes in a monoallelic and mutually exclusive manner. It is conceivable that Bcl11b may regulate this common and unique mode of gene expression. In future experiments, it will be interesting to investigate genomic region tethering of the transcription factor, Bcl11b, using chromatin immunoprecipitation (ChIP) on DNA chip analysis and ChIP sequencing analysis in combination with microarray data to understand the molecular mechanism that underlies the Bcl11b-mediated regulation of VSN development.

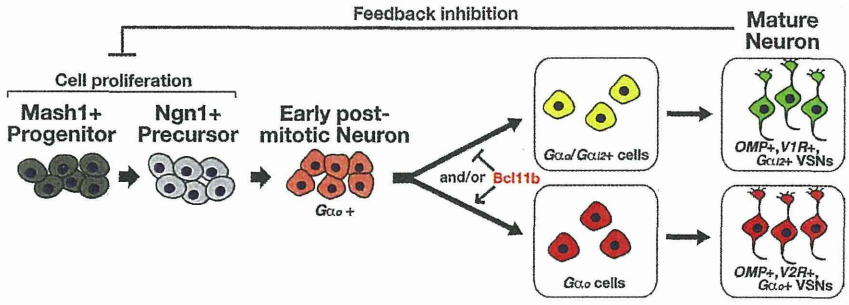

Figure 10. A model of the fate determination of vomeronasal sensory neurons. *Mash1* is required for the generation of both types of VSNs and acts upstream of *Ngn1* and *Bcl11b*. Two types of neurons are segregated from each other and from the common $G\alpha_o$-positive postmitotic neurons. The fate of VSN types is regulated by *Bcl11b* directly or indirectly, and Bcl11b may act as a suppressor for the pathway to the V1r/$G\alpha_{i2}$-positive neurons and/or as an activator for the pathway to the V2r/$G\alpha_o$-positive neurons. In the absence of *Bcl11b*, normal numbers of neurons are produced because Bcl11b is not essential for neurogenesis in the VSN lineage. However, the loss of Bcl11b function disturbs the fate determination balance between the two types of VSNs, which results in increased V1r/$G\alpha_{i2}$-positive neurons and decreased V2r/$G\alpha_o$-positive neurons.

Bcl11b regulates the fate choice between two types of vomeronasal sensory neurons

VSNs can be classified into two major types of neurons: V1r/$G\alpha_{i2}$-positive and V2r/$G\alpha_o$-positive. The fact that both types of VSNs are produced by progenitors in a Mash1-dependent manner and develop side by side in the VNE has raised the question of when their fates are determined and how this dichotomy is regulated. A recent study that used BrdU pulse-labeling experiments suggested that $G\alpha_{i2}$- and $G\alpha_o$-positive neurons mature independently of each other (de la Rosa-Prieto et al., 2010). Our observations provide the different and novel view that the dichotomy of VSNs is regulated by Bcl11b postmitotically. First, we found that all $G\alpha_{i2}$-expressing neurons coexpressed $G\alpha_o$ in the embryonic VNE (Fig. 9*C*), and that this coexpression was observed in the marginal region of the adult VNE, an area where newly differentiated and postmitotic immature neurons are located. Second, $G\alpha_{i2}/G\alpha_o$ double-positive VSNs expressed *V1r*, but not *V2r*, at P0, indicating commitment to the V1r/$G\alpha_{i2}$ VSN lineage. These results suggest that V1r/$G\alpha_{i2}$-type VSNs are generated via $G\alpha_{i2}/G\alpha_o$ double-positive neurons. Third, a small number of $G\alpha_o$-expressing cells colabeled with the differentiating/postmitotic neuron marker *NeuroD*, but none of the $G\alpha_{i2}$-expressing cells were *NeuroD*-positive in the VNE (data not shown), indicating that the expression of $G\alpha_o$ is earlier than $G\alpha_{i2}$ in the course of the differentiation of VSNs. Fourth, we detected the expression of $G\alpha_o$ at E14.5. However, the expression of $G\alpha_{i2}$ was observed later, around E16.5, which indicates that $G\alpha_o$ single-positive cells exist solely in the early development of the VNE. Therefore, it is likely that the early postmitotic neuron first expresses $G\alpha_o$, and then the $G\alpha_{i2}/G\alpha_o$-positive cell is generated for the V1r/$G\alpha_{i2}$ VSN lineage. It is conceivable that $G\alpha_o$-positive neurons may be the default type of VSNs. It is interesting that phylogenetically ancient animals, such as fish and frogs, have larger numbers of *V2r* genes than *V1r* genes (Shi and Zhang, 2007), which suggests that they predominantly use and develop V2r/$G\alpha_o$ VSNs.

In addition, we demonstrated that the loss of Bcl11b function affects the number of two types of VSNs in opposite ways (i.e., the number of $G\alpha_{i2}/G\alpha_o$ double-positive apical VSNs increases, but the number of $G\alpha_o$ single-positive basal VSNs decreases). This phenotype is supported by the additional observation of the expression of *Meis2* and *Tcfap2e*, which are novel identifiers of apical and basal VSNs, respectively. Because the number of cells in the VNE was unaltered in *Bcl11b*$^{-/-}$ mice, it is likely that the balance of the fate choice between the V1r/$G\alpha_{i2}$ and V2r/$G\alpha_o$ VSNs was disturbed by the loss of Bcl11b activity. These results led us to propose a model in which the dichotomy of VSNs is regulated by Bcl11b (Fig. 10). In this model, Bcl11b regulates the fate choice in early postmitotic neurons to determine the type of VSN, either $G\alpha_{i2}$-positive or $G\alpha_o$-positive, by suppressing the $G\alpha_{i2}$-positive pathway and/or activating the pathway for the $G\alpha_o$-positive VSNs. The role of Bcl11b in fate determination has been demonstrated in other systems. In the immune system, Bcl11b is required for early T-cell lineage commitment by the suppression of other pathways for the determination of the fates of natural killer, myeloid, and dendritic cells (Wakabayashi et al., 2003a; Ikawa et al., 2010; Li et al., 2010a,b). In the CNS, Bcl11b is involved in the fate choice of subcortical projection neurons (Chen et al., 2008) and in the pathways of medium spiny neuron specification and differentiation (Arlotta et al., 2008), which suggests a common function of Bcl11b in fate choice during differentiation in different systems by the control of the expression of downstream genes.

Notes

Supplemental material for this article is available at http://www.hirota.bio.titech.ac.jp/publication/JNeuroscience_2011Bcl11b.pdf. Additional images of Bcl11b expression analysis and coexpression analysis of NeuroD with Gαo and Gαi2 are presented. This material has not been peer reviewed.

References

Albu DI, Feng D, Bhattacharya D, Jenkins NA, Copeland NG, Liu P, Avram D (2007) BCL11B is required for positive selection and survival of double-positive thymocytes. J Exp Med 204:3003–3015.

Arlotta P, Molyneaux BJ, Chen J, Inoue J, Kominami R, Macklis JD (2005) Neuronal subtype-specific genes that control corticospinal motor neuron development in vivo. Neuron 45:207–221.

Arlotta P, Molyneaux BJ, Jabaudon D, Yoshida Y, Macklis JD (2008) Ctip2 controls the differentiation of medium spiny neurons and the establishment of the cellular architecture of the striatum. J Neurosci 28:622–632.

Avram D, Fields A, Pretty On Top K, Nevrivy DJ, Ishmael JE, Leid M (2000) Isolation of a novel family of C(2)H(2) zinc finger proteins implicated in transcriptional repression mediated by chicken ovalbumin upstream promoter transcription factor (COUP-TF) orphan nuclear receptors. J Biol Chem 275:10315–10322.

Berghard A, Buck LB (1996) Sensory transduction in vomeronasal neurons: evidence for G α o, G α i2, and adenylyl cyclase II as major components of a pheromone signaling cascade. J Neurosci 16:909–918.

Brennan PA, Zufall F (2006) Pheromonal communication in vertebrates. Nature 444:308–315.

Camoletto P, Colesanti A, Ozon S, Sobel A, Fasolo A (2001) Expression of

stathmin and SCG10 proteins in the olfactory neurogenesis during development and after lesion in the adulthood. Brain Res Bull 54:19–28.
Cau E, Gradwohl G, Fode C, Guillemot F (1997) Mash1 activates a cascade of bHLH regulators in olfactory neuron progenitors. Development 124:1611–1621.
Cau E, Casarosa S, Guillemot F (2002) Mash1 and Ngn1 control distinct steps of determination and differentiation in the olfactory sensory neuron lineage. Development 129:1871–1880.
Chen B, Wang SS, Hattox AM, Rayburn H, Nelson SB, McConnell SK (2008) The Fezf2-Ctip2 genetic pathway regulates the fate choice of subcortical projection neurons in the developing cerebral cortex. Proc Natl Acad Sci U S A 105:11382–11387.
Cherrier T, Suzanne S, Redel L, Calao M, Marban C, Samah B, Mukerjee R, Schwartz C, Gras G, Sawaya BE, Zeichner SL, Aunis D, Van Lint C, Rohr O (2009) p21(WAF1) gene promoter is epigenetically silenced by CTIP2 and SUV39H1. Oncogene 28:3380–3389.
Cismasiu VB, Paskaleva E, Suman Daya S, Canki M, Duus K, Avram D (2008) BCL11B is a general transcriptional repressor of the HIV-1 long terminal repeat in T lymphocytes through recruitment of the NuRD complex. Virology 380:173–181.
Cuschieri A, Bannister LH (1975) The development of the olfactory mucosa in the mouse: light microscopy. J Anat 119:277–286.
de la Rosa-Prieto C, Saiz-Sanchez D, Ubeda-Bañon I, Argandoña-Palacios L, Garcia-Muñozguren S, Martinez-Marcos A (2010) Neurogenesis in subclasses of vomeronasal sensory neurons in adult mice. Dev Neurobiol 70:961–970.
Duggan CD, DeMaria S, Baudhuin A, Stafford D, Ngai J (2008) Foxg1 is required for development of the vertebrate olfactory system. J Neurosci 28:5229–5239.
Dulac C, Axel R (1995) A novel family of genes encoding putative pheromone receptors in mammals. Cell 83:195–206.
Dulac C, Torello AT (2003) Molecular detection of pheromone signals in mammals: from genes to behaviour. Nat Rev Neurosci 4:551–562.
Faedo A, Ficara F, Ghiani M, Aiuti A, Rubenstein JL, Bulfone A (2002) Developmental expression of the T-box transcription factor T-bet/Tbx21 during mouse embryogenesis. Mech Dev 116:157–160.
Garrosa M, Gayoso MJ, Esteban FJ (1998) Prenatal development of the mammalian vomeronasal organ. Microsc Res Tech 41:456–470.
Golonzhka O, Metzger D, Bornert JM, Bay BK, Gross MK, Kioussi C, Leid M (2009a) Ctip2/Bcl11b controls ameloblast formation during mammalian odontogenesis. Proc Natl Acad Sci U S A 106:4278–4283.
Golonzhka O, Liang X, Messaddeq N, Bornert JM, Campbell AL, Metzger D, Chambon P, Ganguli-Indra G, Leid M, Indra AK (2009b) Dual role of COUP-TF-interacting protein 2 in epidermal homeostasis and permeability barrier formation. J Invest Dermatol 129:1459–1470.
Graziadei PP, Levine RR, Graziadei GA (1978) Regeneration of olfactory axons and synapse formation in the forebrain after bulbectomy in neonatal mice. Proc Natl Acad Sci U S A 75:5230–5234.
Guillemot F, Lo LC, Johnson JE, Auerbach A, Anderson DJ, Joyner AL (1993) Mammalian achaete-scute homolog 1 is required for the early development of olfactory and autonomic neurons. Cell 75:463–476.
Halpern M, Martínez-Marcos A (2003) Structure and function of the vomeronasal system: an update. Prog Neurobiol 70:245–318.
Herrada G, Dulac C (1997) A novel family of putative pheromone receptors in mammals with a topographically organized and sexually dimorphic distribution. Cell 90:763–773.
Hirota J, Mombaerts P (2004) The LIM-homeodomain protein Lhx2 is required for complete development of mouse olfactory sensory neurons. Proc Natl Acad Sci U S A 101:8751–8755.
Hirota J, Omura M, Mombaerts P (2007) Differential impact of Lhx2 deficiency on expression of class I and class II odorant receptor genes in mouse. Mol Cell Neurosci 34:679–688.
Ikawa T, Hirose S, Masuda K, Kakugawa K, Satoh R, Shibano-Satoh A, Kominami R, Katsura Y, Kawamoto H (2010) An essential developmental checkpoint for production of the T cell lineage. Science 329:93–96.
Ikeda K, Ookawara S, Sato S, Ando Z, Kageyama R, Kawakami K (2007) Six1 is essential for early neurogenesis in the development of olfactory epithelium. Dev Biol 311:53–68.
Ishii T, Hirota J, Mombaerts P (2003) Combinatorial coexpression of neural and immune multigene families in mouse vomeronasal sensory neurons. Curr Biol 13:394–400.
Ishii T, Omura M, Mombaerts P (2004) Protocols for two- and three-color fluorescent RNA in situ hybridization of the main and accessory olfactory epithelia in mouse. J Neurocytol 33:657–669.
Jia C, Halpern M (1996) Subclasses of vomeronasal receptor neurons: differential expression of G proteins (Gi alpha 2 and G(o alpha)) and segregated projections to the accessory olfactory bulb. Brain Res 719:117–128.
Kaneko-Goto T, Yoshihara S, Miyazaki H, Yoshihara Y (2008) BIG-2 mediates olfactory axon convergence to target glomeruli. Neuron 57:834–846.
Kawauchi S, Kim J, Santos R, Wu HH, Lander AD, Calof AL (2009) Foxg1 promotes olfactory neurogenesis by antagonizing Gdf11. Development 136:1453–1464.
Keverne EB (1999) The vomeronasal organ. Science 286:716–720.
Leid M, Ishmael JE, Avram D, Shepherd D, Fraulob V, Dollé P (2004) CTIP1 and CTIP2 are differentially expressed during mouse embryogenesis. Gene Expr Patterns 4:733–739.
Li L, Leid M, Rothenberg EV (2010a) An early T cell lineage commitment checkpoint dependent on the transcription factor Bcl11b. Science 329:89–93.
Li P, Burke S, Wang J, Chen X, Ortiz M, Lee SC, Lu D, Campos L, Goulding D, Ng BL, Dougan G, Huntly B, Gottgens B, Jenkins NA, Copeland NG, Colucci F, Liu P (2010b) Reprogramming of T cells to natural killer-like cells upon Bcl11b deletion. Science 329:85–89.
Marban C, Suzanne S, Dequiedt F, de Walque S, Redel L, Van Lint C, Aunis D, Rohr O (2007) Recruitment of chromatin-modifying enzymes by CTIP2 promotes HIV-1 transcriptional silencing. EMBO J 26:412–423.
Matsunami H, Buck LB (1997) A multigene family encoding a diverse array of putative pheromone receptors in mammals. Cell 90:775–784.
Murray RC, Navi D, Fesenko J, Lander AD, Calof AL (2003) Widespread defects in the primary olfactory pathway caused by loss of Mash1 function. J Neurosci 23:1769–1780.
Rodriguez I, Del Punta K, Rothman A, Ishii T, Mombaerts P (2002) Multiple new and isolated families within the mouse superfamily of V1r vomeronasal receptors. Nat Neurosci 5:134–140.
Ryba NJ, Tirindelli R (1997) A new multigene family of putative pheromone receptors. Neuron 19:371–379.
Schlüter C, Duchrow M, Wohlenberg C, Becker MH, Key G, Flad HD, Gerdes J (1993) The cell proliferation-associated antigen of antibody Ki-67: a very large, ubiquitous nuclear protein with numerous repeated elements, representing a new kind of cell cycle-maintaining proteins. J Cell Biol 123:513–522.
Senawong T, Peterson VJ, Avram D, Shepherd DM, Frye RA, Minucci S, Leid M (2003) Involvement of the histone deacetylase SIRT1 in chicken ovalbumin upstream promoter transcription factor (COUP-TF)-interacting protein 2-mediated transcriptional repression. J Biol Chem 278:43041–43050.
Shi P, Zhang J (2007) Comparative genomic analysis identifies an evolutionary shift of vomeronasal receptor gene repertoires in the vertebrate transition from water to land. Genome Res 17:166–174.
St John JA, Clarris HJ, McKeown S, Royal S, Key B (2003) Sorting and convergence of primary olfactory axons are independent of the olfactory bulb. J Comp Neurol 464:131–140.
Sullivan SL, Bohm S, Ressler KJ, Horowitz LF, Buck LB (1995) Target-independent pattern specification in the olfactory epithelium. Neuron 15:779–789.
Suzuki Y, Mizoguchi I, Nishiyama H, Takeda M, Obara N (2003) Expression of Hes6 and NeuroD in the olfactory epithelium, vomeronasal organ and non-sensory patches. Chem Senses 28:197–205.
Takami S, Fernandez GD, Graziadei PP (1992) The morphology of GABA-immunoreactive neurons in the accessory olfactory bulb of rats. Brain Res 588:317–323.
Topark-Ngarm A, Golonzhka O, Peterson VJ, Barrett B Jr, Martinez B, Crofoot K, Filtz TM, Leid M (2006) CTIP2 associates with the NuRD complex on the promoter of p57KIP2, a newly identified CTIP2 target gene. J Biol Chem 281:32272–32283.
Wakabayashi Y, Inoue J, Takahashi Y, Matsuki A, Kosugi-Okano H, Shinbo T, Mishima Y, Niwa O, Kominami R (2003a) Homozygous deletions and point mutations of the Rit1/Bcl11b gene in gamma-ray induced mouse thymic lymphomas. Biochem Biophys Res Commun 301:598–603.
Wakabayashi Y, Watanabe H, Inoue J, Takeda N, Sakata J, Mishima Y, Hitomi J, Yamamoto T, Utsuyama M, Niwa O, Aizawa S, Kominami R (2003b) Bcl11b is required for differentiation and survival of alphabeta T lymphocytes. Nat Immunol 4:533–539.
Yoshihara S, Omichi K, Yanazawa M, Kitamura K, Yoshihara Y (2005) Arx homeobox gene is essential for development of mouse olfactory system. Development 132:751–762.

Cellular Signalling 24 (2012) 1047–1052

Contents lists available at SciVerse ScienceDirect

Cellular Signalling

journal homepage: www.elsevier.com/locate/cellsig

BCL11B tumor suppressor inhibits *HDM2* expression in a p53-dependent manner

Miki Obata, Ryo Kominami, Yukio Mishima *

Department of Molecular Genetics, Niigata University Graduate School of Medical and Dental Sciences, 1-757 Asahimachi-dori, Chuo-ku, Niigata 951-8510, Japan

ARTICLE INFO

Article history:
Received 4 November 2011
Received in revised form 13 December 2011
Accepted 31 December 2011
Available online 5 January 2012

Keywords:
BCL11B
HDM2
p53
p53-HDM2 feedback loop
Tumor suppressor

ABSTRACT

BCL11B is a C_2H_2 zinc finger transcription factor that acts as a haploinsufficient tumor suppressor. Mutations and deletion in the human orthologue *BCL11B* have been identified in human T-cell acute lymphoblastic leukemia (T-ALL) and a mouse model of thymic lymphomas. *Bcl11b*$^{KO/+}$*p53*$^{KO/+}$ doubly heterozygous mice, but not *Bcl11b*$^{KO/+}$ heterozygous mice, spontaneously develop thymic lymphomas at a high frequency, suggesting cooperativity of BCL11B and p53 in cancer development. In this study, we have examined whether or not BCL11B directly affects the p53 signaling pathway including HDM2, a ubiquitin ligase for p53 degradation. The p53 pathway regulates cell proliferation and the response to DNA damages to maintain genome integrity. Here we show that BCL11B binds to human *HDM2*-P2 promoter by ChIP (chromatin immuno-precipitation) assay and inhibits HDM2 expression in a p53-dependent manner. Deletion of the distal p53 responsive element in *HDM2* promoter region or the lack of p53 in HCT116 cells greatly reduced the repressive effect of BCL11B on *HDM2*-P2 promoter activity. The repressive activity was alleviated in γ-ray induced DNA damage conditions that activate p53, suggesting interaction between BCL11B and p53 for *HDM2* expression. These date suggest that BCL11B affects the activity of the p53-HDM2 feedback loop in basal and irradiated conditions. This may be a mechanism underlying the leukemic transformation in T-ALL and in *Bcl11b*$^{KO/+}$*p53*$^{KO/+}$ mouse thymocytes.

1. Introduction

The E3 ubiquitin ligase HDM2 (human homologue of MDM2, mouse double minute 2) and the tumor suppressor p53 form a negative feedback loop, a balanced regulatory network of proteins that controls cell cycle progression and commitment to apoptosis [1,2]. When cells undergo γ-irradiation that induces DNA damages, p53 proteins increase by phosphorylation, which in turn activates transcription of *HDM2* leading to p53 degradation. Thus, HDM2 acts as a negative regulator of p53. HDM2 binds to several other proteins such as p14^{ARF} and ribosomal protein RPL26, positive regulators of p53, and their degradation also leads to downregulation of p53 [1,2]. As for *HDM2* transcription, AP-1, Ets and Smad2/3 activate the transcription in a p53-independent manner under oncogenic pathways such as the growth factor TGFβ [2,3]. *HDM2* transcription is regulated at two distinct promoters of P1 and P2 [2–8], and P1 promoter is located upstream of the first exon of the *HDM2* gene whereas P2 promoter is situated within the first intron. P1 promoter controls basal expression of *HDM2*, and P2 promoter is highly regulated through multiple response elements within the promoter [2,3]. An activation of P2 promoter occurs via p53 in response to DNA damage agents such as γ-radiation [7,8].

Bcl11b (B cell leukemia/lymphoma-11b), also known as *Rit1* and *CTIP2*, belongs to a C_2H_2 zinc-finger transcription factor [9,10]. *Bcl11b* is expressed in various tissues including thymocytes [10–14], neurons [15,16], skin [17] and tooth [18], exhibiting critical roles in development of those organ systems. BCL11B is identified as a transcriptional repressor [19,20] by mediating either directly binds to a GC-rich consensus sequence of target genes including *p21* and *p57* and/or interacts with nucleosome remodeling and histone deacetylase (NuRD) complex [21,22].

Bcl11b was originally identified as a tumor suppressor gene in mouse thymic lymphomas, a model of human T-cell acute lymphoblastic leukemia (T-ALL) [10,23,24]. Recently, mutations and deletion of *BCL11B* have been identified in T-ALL [25–28]. Although *Bcl11b*$^{KO/KO}$ knockout mice die shortly after birth, *Bcl11b*$^{KO/+}$ heterozygous mice rarely develop thymic lymphomas [24]. However, *Bcl11b*$^{KO/+}$*p53*$^{KO/+}$ doubly heterozygous mice develop thymic lymphomas at a high frequency [23]. This suggests cooperativity between BCL11B and p53 in cancer development. In this study, we have addressed this issue by examining whether or not BCL11B directly affects the p53 and HDM2 feedback loop. Here we show that BCL11B directly interacts with P2 promoter region of *HDM2* and inhibits *HDM2* promoter activity in a p53-dependent manner.

2. Materials and methods

2.1. Plasmid construction

Bcl11b coding sequences were cloned into pcDNA3.1 (Invitrogen) as described previously [10]. Lentivirus vectors expressing shRNA for

* Corresponding author. Tel.: +81 25 227 2082; fax: +81 25 227 0757.
E-mail address: ymishima@med.niigata-u.ac.jp (Y. Mishima).

0898-6568/$ – see front matter © 2012 Elsevier Inc. All rights reserved.
doi:10.1016/j.cellsig.2011.12.026

BCL11B and full-length *Bcl11b* were constructed using BLOCK-iT lentiviral Pol II miR RNAi expression system (Invitrogen). Target sequence for *BCL11B* was described previously [29]. Promoter fragments of *HDM2* were amplified from genomic DNA of Jurkat and MOLT-4 cells and inserted into the NheI and HindIII sites of pGL3-Basic plasmid (Promega). DNAs from Jurkat cells and MOLT-4 cells carry wild-type sequence (T) and the SNP sequence (G) (the 309th nucleotide in the first intron), respectively [30]. Primers used for the *HDM2*-P1 and *HDM2*-P2 driven luciferase reporter plasmids are listed in the Supplementary Table 1. *HDM2*-P2 deletion mutants were generated using primeSTAR mutagenesis basal kit (Takara) by using primer sets listed in the Supplementary Table 1.

2.2. Cell culture, transfection and luciferase assays

Human T cell line Jurkat (p53 deficient) and MOLT-4 (p53 wild) cells were cultured in RPMI-1640 medium containing 10% fetal bovine serum (FBS) (Nitirei). For recombinant lentivirus production, HEK293FT cells were used according to the protocol recommended by the manufacturer (Invitrogen).

HCT116 ($p53^{+/+}$ or $p53^{-/-}$) cells were cultured in DMEM medium (Sigma), supplemented with 10% FBS (Nitirei). The HCT116 ($p53^{-/-}$) cell line was kindly provided by Drs. B. Vogelstein and K.W. Kinzles (Johns Hopkins University). All transfections were performed with FuGENE 6 Reagent (Roche) according to the manufacturer's instructions. HCT116 ($p53^{+/+}$ or $p53^{-/-}$) cells were grown in 12-well plate. Plasmid DNA expressing wild-type BCL11B and indicated *HDM2* promoter-driven *Photinus pyralis* luciferase reporter plasmid (Promega) were transfected the next day. Cells were lysed after 24 h using luciferase lysis buffer (Toyo Ink), and luciferase activities were measured using the Dual-luciferase-reporter system according to the manufacturer's instructions. Transfection efficiency in luciferase reporter assays was controlled and normalized by including a constant amount of *TK-Renilla reniformis* luciferase reporter plasmid in all transfections. The activity is mostly expressed in the percent of wild-type BCL11B versus the BCL11B del Z4-6 mutant lacking activity (BCL11B del Z4-6; deleted C-terminal three zinc finger domains). The data shown were of three independent triplicate experiments as the mean ± standard deviations (SD) of the ratio between the *Photinus* and *Renilla* reporters.

γ-irradiation (10–15 Gy) was performed using a Cs^{137} irradiator.

2.3. RT-PCR

Total RNA was prepared from Jurkat, MOLT-4 or HCT116 cells by the RNA Easy Mini kit (Quiagen) according to the protocol recommended by the manufacturer. cDNA was synthesized from 5 μg of total RNA with a random primer using SuperScript II reverse transcriptase (Invitrogen) and a 10-fold dilution aliquot was used for PCR using primers described in the Supplementary Table 2. PCR program was: 1 min at 94 °C, followed by 32 cycles (30 s at 94 °C, 30 s at 54 °C, 1 min at 72 °C), followed by 5 min extension at 72 °C. PCR products were separated by 5% polyacrylamide gel electrophoresis (PAGE) and visualized as bands by staining with ethidium bromide. The intensity of bands was analyzed with Molecular Imager FX (Bio-Rad). Comparison in the band intensity was done between pLent-sh*SC* and pLent-sh*BCL11b* transfected MOLT4 cells or between pLent-*GFP* and pLent-*Bcl11b* transfected HCT116 cells.

2.4. Western blot analysis

Western blotting was performed as previously described [29]. Antibodies used were rabbit anti-BCL11B-Z [11], anti-MDM2 (R & D Systems, AF1244), anti-p53 (Cell Signaling, #2524), anti-ACTIN (Santa Cruz, sc-1615), HRP (horseradish peroxidase)-anti-goat IgG (Santa Cruz, sc-2020), HRP-anti-rabbit IgG (GE Healthcare Amersham, NA-934) and HRP-anti-mouse IgG (GE Healthcare Amersham, NA-931). Protein bands were visualized using chemiluminescent detection (ECL plus, GE Healthcare Amersham), and the intensity of bands was analyzed with Molecular Imager FX (Bio-Rad). The protein levels are shown relative to ACTIN used as a control, and are compared between pLent-sh*SC* and pLent-sh*BCL11b* transfected MOLT4 cells or between pLent-*GFP* and pLent-*Bcl11b* transfected HCT116 cells.

2.5. Chromatin immunoprecipitation

Chromatin immunoprecipitation (ChIP) assay was performed using a ChIP assay kit (#17-295; Milopore, Upstate). Briefly, MOLT-4 and Jurkat cells were fixed with formaldehyde and sonicated. The collected chromatin solutions were incubated with anti- BCL11B antibodies (Abcom ab18465) or normal IgG (Immuno Biological Laboratories, Co. Ltd., Japan 17312) at 4 °C overnight. The immunoprecipitated complexes were eluted followed by removal of cross-links. The resulting immunoprecipitated DNA and input DNA (1% of total DNA) were subjected to PCR using primer sets described in the Supplementary Table 3. PCR products were separated by 5% PAGE and visualized by staining with ethidium bromide.

2.6. Statistical analyses

Data from at least three independent experiments were analyzed for statistical significance by Student's *t*-test. All values are expressed as mean ± SD and the value of $P<0.01$, shown by *, was considered statistically significant.

3. Results

3.1. BCL11B suppresses HDM2-P2 promoter activity

MOLT-4 cells highly expressed BCL11B but expressed HDM2 and p53 at low levels in basal conditions. We introduced pLent-sh*BCL11B* or control pLent-sh*SC* viruses into the MOLT-4 cells and examined changes in the expression of HDM2 and p53 in *BCL11B*-knockdown (KD) MOLT-4 cells. KD cells showed an increase in expression of HDM2 but not of p53 (Fig. 1A). Supplementary Fig. 1A shows failure in the specific binding of BCL11B to p53 promoter, which indicated no effect of BCL11B on p53 transcription (Supplementary Fig. 1B). Fig. 1B shows the location of P1 and P2 promoters in *HDM2* gene [2–8]. KD cells showed an increase in RNA transcripts from P2 promoter but not from P1 promoter (Fig. 1C). Supplementary Fig. 2A shows a γ-ray induced increase in RNA transcripts from P2 promoter but not from P1 promoter, and Supplementary Fig. 2B shows γ-ray induced stabilization of p53 but no change in expression of BCL11B or HDM2 proteins. These results demonstrated that reduced expression of BCL11B in MOLT-4 cells resulted in upregulation of *HDM2* transcription and that γ-irradiation affected p53 expression but not BCL11B or HDM2 expression.

We next examined BCL11B effect in HCT116 cells, which expressed HDM2 and p53 but not BCL11B. We infected viruses introducing BCL11B expression (pLent-*Bcl11b*) and control viruses (pLent-*GFP*) to HCT116 cells, and examined expressions of HDM2 and p53. Over-expression of BCL11B reduced HDM2 expression at the protein and RNA levels (Fig. 1D and E, respectively). These results suggest that BCL11B downregulates *HDM2* transcription in HCT116 cells, consistent with the repressor activity of BCL11B for *HDM2* expression found in *BCL11B*-KD MOLT-4 cells.

3.2. BCL11B binds to HDM2 promoter

To examine whether or not BCL11B associates with *HDM2* P2 promoter, we performed chromatin immunoprecipitaion (ChIP) assay in MOLT-4 and Jurkat cells expressing BCL11B. Five sets of primers were

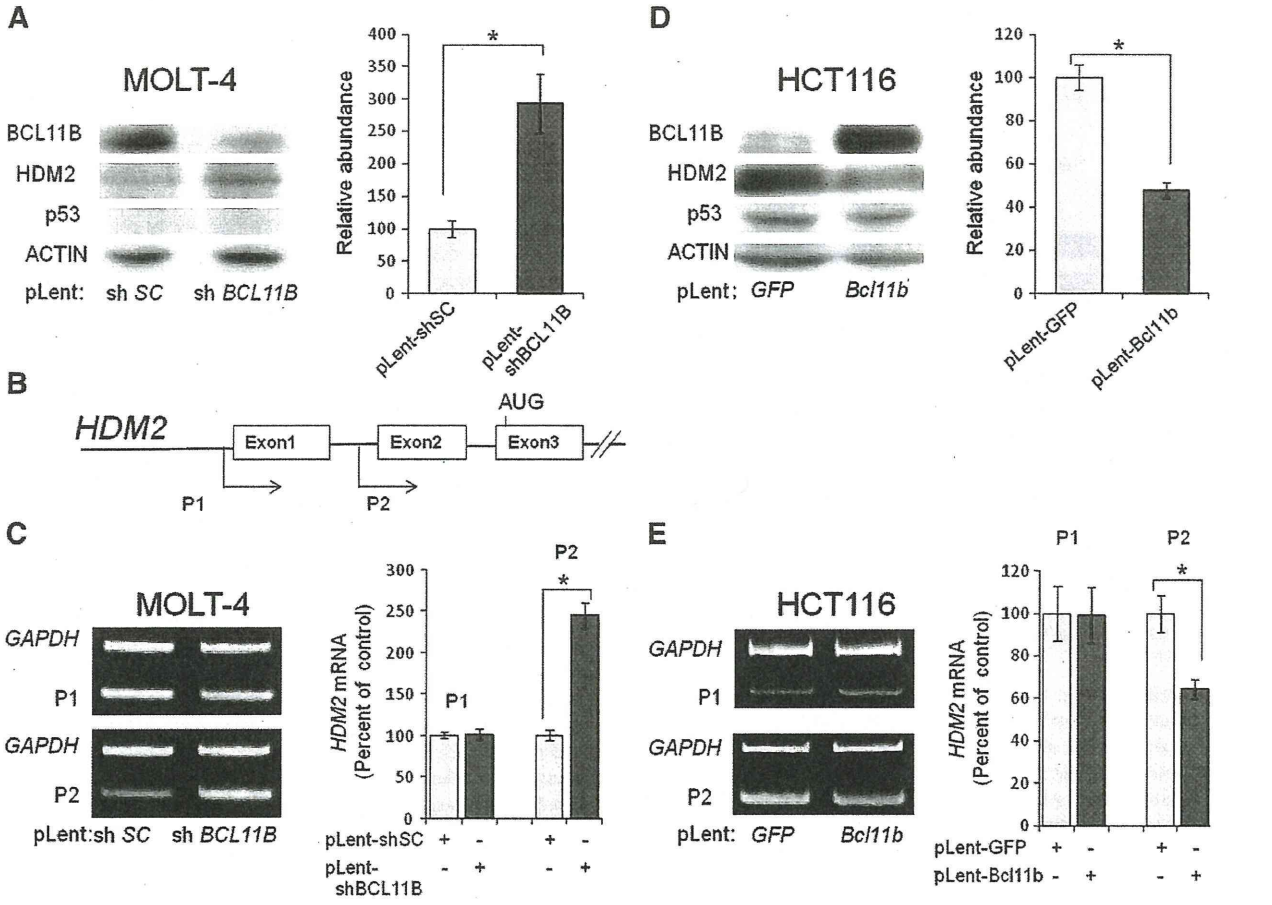

Fig. 1. BCL11B reduces *HDM2* expression by inhibiting *HDM2* promoter activity. (A) Protein expression levels in MOLT-4 cells that were transduced with control (pLent-sh*SC*) or lentivirus vector expressing shRNA for BCL11B (pLent-sh*BCL11B*) were analyzed by Western blotting at 6 days after transduction. The graph in the right shows a significant difference of HDM2 levels between pLent-sh*SC* and pLent-sh*BCL11B*. * indicates P<0.01. The levels are shown relative to ACTIN used as a control. (B) Schematic representation of *HDM2*-P1 and *HDM2*-P2 promoters. (C) RT-PCR analysis of *HDM2* RNA expression levels in treated cells as in (A). The graph shows comparison of *HDM2* mRNA levels transcribed from P1 and P2 promoters between pLent-sh*SC* and pLent-sh*BCL11B*. The mRNA levels are shown relative to *GAPDH* used as an internal control. * indicates P<0.01. (D) Protein expression levels in HCT116 cells that were transduced with control (pLent-*GFP*) or lentivirus vector expressing BCL11B (pLent-*Bcl11b*) were analyzed by Western blotting at 48 h after transduction. The graph shows comparison of *HDM2* protein levels as in (A). * indicates P<0.01. (E) RT-PCR analysis of *HDM2* RNA expression levels in treated cells as in (D). The graph shows comparison of *HDM2* mRNA levels. * indicates P<0.01. Data are presented as the mean ± SD.

used in different positions encompassing the promoter site (Fig. 2A). DNA fragments of P2 promoter region were enriched in the precipitant by BCL11B antibodies in both cell lines, whereas 5′-upstream and 3′-downstream regions were not enriched (Fig. 2B). Primers for control regions on *β-ACTIN* or on *IL-7R* genes did not show enrichment either. These results suggest that BCL11B directly binds to the *HDM2*-P2 promoter region.

3.3. *BCL11B inhibits HDM2-P2 promoter activity in a p53-dependent manner*

To further characterize the repressor activity of BCL11B for *HDM2* expression, we performed a luciferase reporter gene assay in *p53*-proficient HCT116 cells and *p53*-lacking HCT116 cells. We used two kinds of *HDM2*-P2 promoter sequences for the construct carrying wild-type T sequence at the 309th nucleotide position in the first intron and the variant G sequence at the position, because the variant-309 P2 promoter was reported to have a higher promoter activity by enhancing the binding of transcription factor Sp1 [30]. Transfection of BCL11B expression vector showed that BCL11B strongly inhibited the activity of both wild-type and variant *HDM2*-P2 promoters in HCT116 cells (Fig. 3A). The inhibition levels (about 20% of the control for each) were similar between wild-type and variant promoters, which was different from the initial prediction. Inhibition was also detected in p53-lacking HCT116 cells though it was less efficient (about 58% of the control). In contrast, BCL11B expression did not inhibit *HDM2*-P1 promoter activity in either cell line (Fig. 3A). These results suggest that BCL11B inhibits *HDM2* expression by suppressing the *HDM2*-P2 promoter activity and this suppression depends on p53 expression.

There are two p53-binding elements within the *HDM2*-P2 promoter that affect P2 promoter activation [4,5]. We generated five deletion constructs of *HDM2*-P2 promoter region, two of which lacked one of the two elements and one lacked both the p53 responsive elements (Fig. 3B). The construct lacking only proximal p53-binding element (Del-4) retained the promoter activity, suggesting no requirement of the proximal p53 binding element for promoter activity, whereas the construct lacking both elements (Del-5) showed a severe decrease to about 5% of the wild type activity (Fig. 3C). This decrease may be due to lack of the distal p53 binding element. The remaining three mutants showed decreases to 37–58%. Those decreases may be ascribed to lack of binding by other transcription factors than p53 such as AP-1, Ets and Smad2/3 [2,3]. These results suggest that *HDM2*-P2 promoter requires the distal p53 responsive element for

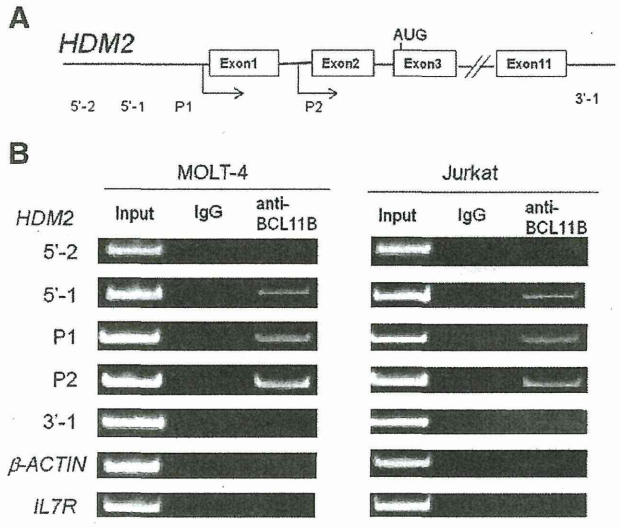

Fig. 2. BCL11B associates with the *HDM2* promoter. (A) Schematic representation of the *HDM2* gene region and positions of PCR primers used (Supplementary Table 3). (B) PCR products for input and ChIP-precipitaed DNA were separated on 5% PAGE and stained with ethidium bromide. Formaldehyde treated MOLT-4 and Jurkat cells were subjected to ChIP using antibodies against BCL11B. *β-ACTIN* gene and *IL7R* promoter were used as negative controls.

efficient transcription, though full activity of the promoter requires other sequence region in addition to the distal element.

We examined the effect of BCL11B on *HDM2*-P2 promoter using those deletion constructs. BCL11B failed to repress P2 promoter activity in the construct lacking both p53 responsive elements, whereas BCL11B efficiently repressed the activity in the three constructs retaining the distal p53 responsive element (Fig. 3D). Of note, the construct (Del-3) lacking the distal p53 responsive element possessed an intermediate activity. These results suggest that the distal element is required and plays a key role for the repression activity by BCL11B, consistent with that BCL11B suppresses the activity of the *HDM2*-P2 promoter in a p53-dependent manner.

3.4. BCL11B suppresses HDM2-P2 promoter with a less efficiency after DNA damages conditions

We examined the effect on *HDM2* expression of γ-irradiation that stabilize and activate p53 activity. We transfected the *HDM2* luciferase reporter vector into p53-proficient and p53-lacking HCT116 cells, and 4 h later those cells were exposed with and without 10 Gy of γ-irradiation. Twenty hours after, we measured the luciferase activity. *HDM2*-P2 promoter but not *HDM2*-P1 promoter activity was increased in response to γ-irradiation in both HCT116 cells (Fig. 4A). This suggests that *HDM2*-P2 promoter is activated by γ-irradiation and the activation is both p53 dependent and p53 independent. The result may be compatible with elevated RNA expressions in MOLT-4 (p53 proficient) and Jurkat (p53 deficient) cells after γ-irradiation (see Supplemental Fig. 2). However, the promoter activity in HCT116 cells was almost 10-fold higher than that in p53-lacking HCT116 cells, suggesting that p53-dependent activation has more impact than p53-independent one.

We next examined BCL11B repressor activity in DNA damage conditions induced by γ-irradiation (Fig. 4B). BCL11B expression inhibited the *HDM2*-P2 promoter activity in p53-proficient HCT116 cells, though the inhibition (about 38% of the control) was less than that (20%) in unirradiated basal conditions (see Fig. 3A). As in p53-lacking HCT116 cells, inhibition by BCL11B was also much less efficient (about 57% of the control), similar to that in unirradiated conditions. These demonstrated a reduced efficiency of BCL11B attenuation for *HDM2* promoter activity in radiation-induced DNA damage conditions. This suggests cooperativity between BCL11B and p53 on *HDM2* promoter activity.

4. Discussion

HDM2 downregulates p53 proteins whereas p53 activates transcription of *HDM2*, which is called the HDM2-p53 feedback loop. In this paper, we have examined the effect of BCL11B on the feedback loop and demonstrated that BCL11B negatively regulates the *HDM2* transcription mainly in a p53-dependent manner in basal conditions. The suppression of *HDM2* transcription may be mostly through the distal p53-binding element in *HDM2* promoter region, because only loss of the distal element alleviated the effect of BCL11B. We observed the repressor activity of BCL11B also in radiation-induced DNA damage conditions that activate p53. However, in the conditions the suppression activity by BCL11B was weaker than that in basal conditions. This suggests competitive interaction present between the activated p53 and BCL11B in the effect on *HDM2* promoter activity.

Gene repression plays an important role in controlling cell differentiation and proliferation [31]. Repression usually depends on sequence-specific DNA-binding repressors that recruit nuclear cofactors termed corepressors, which are directly responsible for silencing transcription [32]. The majority of known corepressors are components of multiprotein complexes that possess enzymatic activities such as deacetylation of histone tails and ATP-dependent remodeling of chromatin [33]. BCL11B acts as a transcriptional repressor [19,20] probably by binding to a GC-rich consensus sequence (GGCCGG) of target genes including the cyclin-dependent kinase inhibitors *p21* and *p57* [21,22]. BCL11B is also known to be associated with a nucleosome remodeling and histone deacetylase (NuRD) [20,21]. There are two GGCCGG sequence motifs within the *HDM*-P2 promoter (287 and 388 relative to the first nucleotide of intron 1). However, those motifs do not seem to serve for BCL11B function, because our results showed that the deletion mutant lacking the motifs (see Del-2 in Fig. 3B) underwent BCL11B-mediating repression. This suggests that BCL11B acts through other *HDM*-P2 promoter region including the distal p53-binding element. Corepressors have been generally considered to be ubiquitous proteins that are subject to little regulation. BCL11B may be included in a group of proteins subject to little regulation, because its expression was not affected in response to γ-irradiation.

p53 and HDM2 are both regulated in response to signals on oncogenic and tumor suppressor pathways. A variety of stress signals regulate p53 and result in p53 stabilization through preventing its degradation by HDM2. p53 is known to transcriptionally activate *HDM2* expression but there are other transcription factors such as AP-1, Ets and Smad2/3 that regulate *HDM2* expression in a p53-independent manner [2,3]. Signaling via Ras and the Erk pathway results in the binding of both AP-1 and Ets family members to a response element in *HDM*-P2 promoter that is immediately adjacent to the p53 responsive elements [2,3,6]. TGFβ has been shown to regulate HDM2 expression via the interaction of Smad2/3 with an element in *HDM*-P2 promoter as well [2]. Another regulator is $p14^{ARF}$ (the product of the alternate reading frame in *INK4A*, $p19^{ARF}$ in mice) that negatively regulates HDM2 at the protein level. $p14^{ARF}$ binds to HDM2 protein, and this binding inhibits the E3 ligase activity of HDM2.

A question on how BCL11B contributes to *HDM2* transcription remains. Since BCL11B expression seems to be not markedly regulated, BCL11B may be a constitutive component participating in the p53-HDM2 feedback loop and differs from regulatory proteins such as p53, AP-1, Ets and Smad2/3. One possible hypothesis is that BCL11B or possibly NuRD complex comprising BCL11B exists near the distal p53-binding element region in basal and irradiated conditions and maintains the alleviated *HDM2* transcription. Loss or decrease of BCL11B abrogates the alleviation, leading to increased HDM2

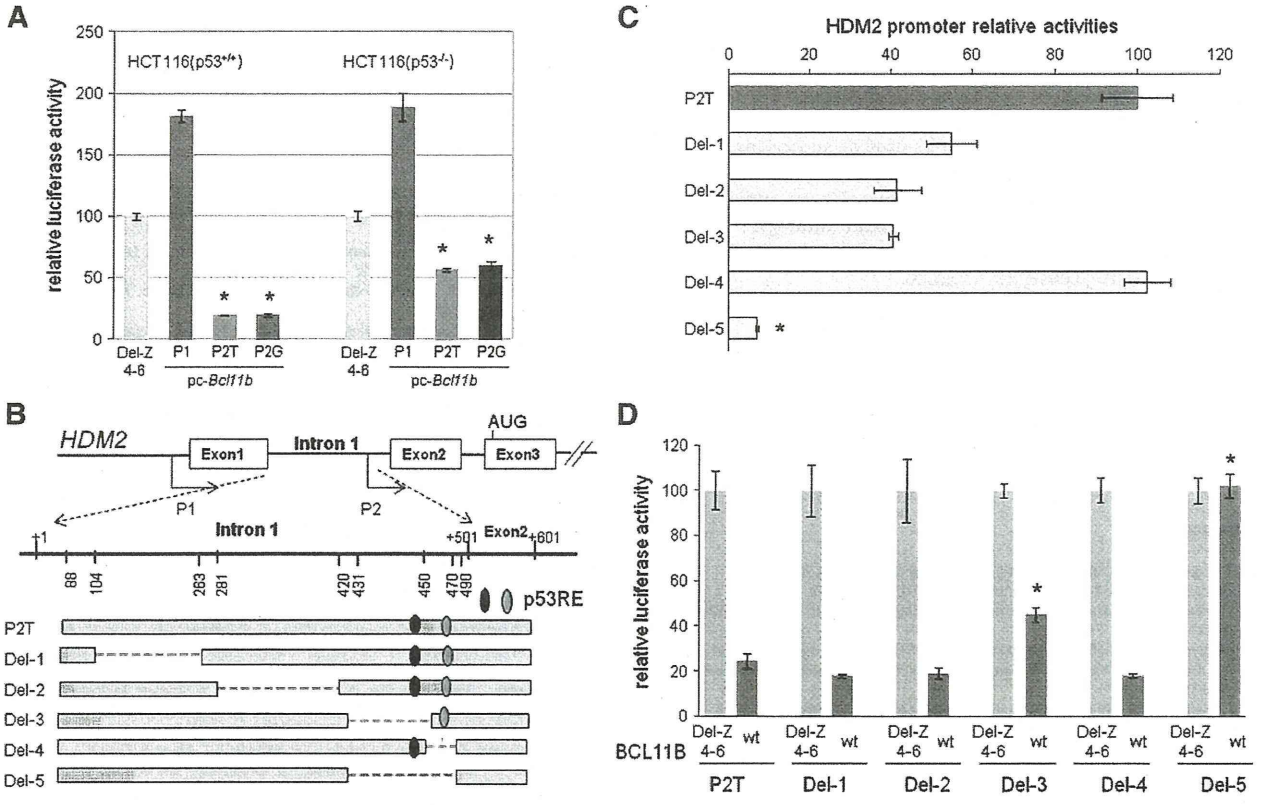

Fig. 3. Inhibition of *HDM2* transcription by BCL11B is dependent on p53. (A) Relative luciferase activities of *HDM2*-P1 and *HDM2*-P2 promoters are shown in HCT116 ($p53^{+/+}$) and HCT116 ($p53^{-/-}$) cells. The activity is expressed in the percent of wild-type BCL11B versus the del Z4-6 mutant lacking BCL11B activity (del Z4-6; deleted C-terminal three zinc finger domains of BCL11B). * indicates $P<0.01$. (B) Schematic representation of *HDM2*-P2 promoter deletion constructs. The distal p53 responsive element is shown as black oval and the proximal p53 responsive element is as gray oval. Nucleotide numbers relative to the first nucleotide (+1) of the first intron of *HDM2* gene are indicated. Del-2 construct lacks the two GGCCGG sequence elements, a putative motif for BCL11B binding. (C) Promoter activity of each deletion mutant is shown relative to P2T construct. * indicates $P<0.01$ (between P2T and Del-5). (D) Relative luciferase activities are shown as in (A). Data are presented as the mean ± SD. * indicates $P<0.01$ (comparison between P2T and Del-3, and between P2T and Del-5).

expression and p53 inactivation. When p53 is activated, p53 activator complex may replace or inactivate the BCL11B repressor complex leading to the activation of *HDM2* promoter.

Bcl11b was originally identified as a haploinsufficient tumor suppressor gene in mouse thymic lymphomas, a model of T-ALL [10,23,24]. Recently, haploinsufficiency has been also observed in T-ALL [27,28]. Another well-known haploinsufficient tumor suppressor is p53 [34]. Of note, $Bcl11b^{KO/+}$ heterozygosity alone gives a weak effect on development of thymic lymphomas, but its effect increases in the $p53^{KO/+}$ heterozygous genetic background [23]. This genetic evidence suggests cooperativity between BCL11B and p53 in lymphoma development.

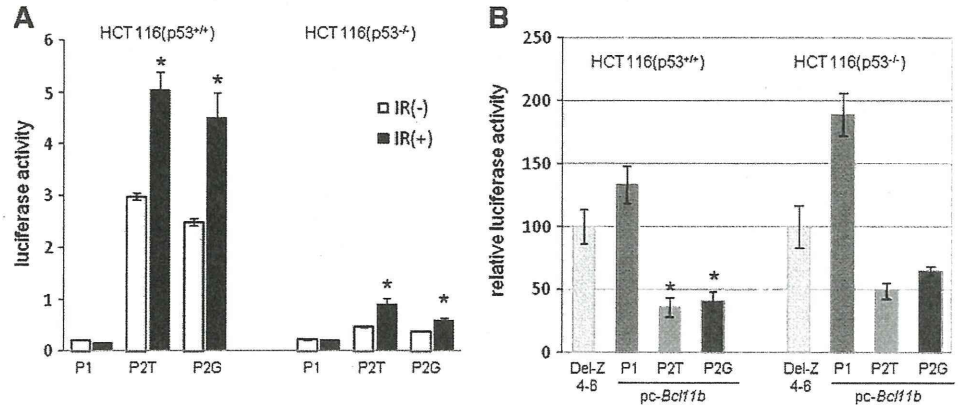

Fig. 4. Attenuation of BCL11B suppression activity for *HDM2* transcription after γ-irradiation. (A) Normalized luciferase activities of *HDM2*-P1 and *HDM2*-P2 promoters after γ-irradiation are shown in HCT116 ($p53^{+/+}$) and HCT116 ($p53^{-/-}$) cells. *HDM2* promoter-driven plasmid was transfected into HCT116 ($p53^{+/+}$) and HCT116 ($p53^{-/-}$) cells, and 4 h later those cells were exposed with and without 10 Gy of γ-irradiation. After 24 h, the luciferase activity was measured. Open columns show unirradiated cells and filled columns indicated irradiated cells. Data are presented as the mean ± SD. * indicates $P<0.01$ (between unirradiated and irradiated cells). (B) Relative luciferase activities after γ-irradiation are shown in HCT116 ($p53^{+/+}$) and HCT116 ($p53^{-/-}$) cells. *HDM2* luciferase reporter vector was transfected together with and without the BCL11B expression vector into HCT116 ($p53^{+/+}$) and HCT116 ($p53^{-/-}$) cells, and 4 h later those cells were exposed to 10 Gy of γ-irradiation. The luciferase activity was measured 24 h after the exposure. The inhibition in HCT116 ($p53^{+/+}$) cells (38% in average of P2T and P2G) was less than that (20%) in unirradiated cells in Fig. 3A (*$P<0.01$).

5. Conclusions

We found that BCL11B binds to human *HDM2*-P2 promoter and inhibits HDM2 expression in a p53-dependent manner. The repressive activity was alleviated in γ-ray induced DNA damage conditions that activate p53. Therefore, our results provide supporting evidence for the cooperativity between BCL11B and p53 in lymphomagenesis. These findings will help better understanding of T-ALL and other cancer pathogenesis and give a clue for therapeutic strategy.

Supplementary materials related to this article can be found online at doi: 10.1016/j.cellsig.2011.12.026.

Acknowledgments

We thank Drs. B. Vogelstein and K.W. Kinzles (Johns Hopkins University) for providing HCT116 ($p53^{-/-}$) cells. This study was supported by grants-in-aid from the Ministry of Education, Science, Technology, Sports, and Culture of Japan.

References

[1] B. Vogelstein, D. Lane, A.J. Levine, Nature 408 (2000) 307–310.
[2] J.J. Manfredi, Genes & Development 24 (2010) 1580–1589.
[3] M. Phelps, M. Darley, J.N. Primrose, J.P. Blaydes, Cancer Research 63 (2003) 2616–2623.
[4] T. Juven, Y. Barak, A. Zauberman, D.L. George, M. Oren, Oncogene 8 (1993) 3411–3416.
[5] A. Zauberman, D. Flusberg, Y. Haupt, Y. Barak, M. Oren, Nucleic Acids Research 23 (1995) 2584–2592.
[6] X. Tian, Y. Chen, W. Hu, M. Wu, Cellular Signalling 23 (2011) 193–200.
[7] Y. Barak, E. Gottlieb, T. Juven-Gershon, M. Oren, Genes & Development 8 (1994) 1739–1749.
[8] W. Duan, L. Gao, X. Wu, Y. Zhang, G.A. Otterson, M.A. Villalona-Calero, Experimental Cell Research 312 (2006) 3370–3378.
[9] D. Avram, A. Fields, K. Pretty On Top, D.J. Nevrivy, J.E. Ishmael, M. Leid, The Journal of Biological Chemistry 275 (2000) 10315–10322.
[10] Y. Wakabayashi, J. Inoue, Y. Takahashi, A. Matsuki, H. Kosugi-Okano, T. Shinbo, Y. Mishima, O. Niwa, R. Kominami, Biochemical and Biophysical Research Communications 301 (2003) 598–603.
[11] Y. Wakabayashi, H. Watanabe, J. Inoue, N. Takeda, J. Sakata, Y. Mishima, J. Hitomi, T. Yamamoto, M. Utsuyama, O. Niwa, S. Aizawa, R. Kominami, Nature Immunology 4 (2003) 533–539.
[12] P. Li, S. Burke, J. Wang, X. Chen, M. Ortiz, S.C. Lee, D. Lu, L. Campos, D. Goulding, B.L. Ng, G. Dougan, B. Huntly, B. Gottgens, N.A. Jenkins, N.G. Copeland, F. Colucci, P. Liu, Science 329 (2010) 85–89.
[13] L. Li, M. Leid, E.V. Rothenberg, Science 329 (2010) 89–93.
[14] T. Ikawa, S. Hirose, K. Masuda, K. Kakugawa, R. Satoh, A. Shibano-Satoh, R. Kominami, Y. Katsura, H. Kawamoto, Science 329 (2010) 93–96.
[15] P. Arlotta, B.J. Molyneaux, J. Chen, J. Inoue, R. Kominami, J.D. Macklis, Neuron 45 (2005) 207–221.
[16] P. Arlotta, B.J. Molyneaux, D. Jabaudon, Y. Yoshida, J.D. Macklis, The Journal of Neuroscience 28 (2008) 622–632.
[17] O. Golonzhka, X. Liang, N. Messaddeq, J.M. Bornert, A.L. Campbell, D. Metzger, P. Chambon, G. Ganguli-Indra, M. Leid, A.K. Indra, Journal of Investigative Dermatology 129 (2008) 1459–1470.
[18] O. Golonzhka, D. Metzger, J.M. Bornert, B.K. Bay, M.K. Gross, C. Kioussi, M. Leid, Proceedings of the National Academy of Sciences of the United States of America 106 (2009) 4278–4283.
[19] D. Avram, A. Fields, T. Senawong, A. Topark-Ngarm, M. Leid, The Biochemical Journal 368 (2002) 555–563.
[20] V.B. Cismasiu, K. Adamo, J. Gecewicz, J. Duque, Q. Lin, D. Avram, Oncogene 24 (2005) 6753–6764.
[21] T. Cherrier, S. Suzanne, L. Redel, M. Calao, C. Marban, B. Samah, R. Mukerjee, C. Schwartz, G. Gras, B.E. Sawaya, S.L. Zeichner, D. Aunis, C. Van Lint, O. Rohr, Oncogene 28 (2009) 3380–3389.
[22] A. Topark-Ngarm, O. Golonzhka, V.J. Peterson, B. Barrett Jr., B. Martinez, K. Crofoot, T.M. Filtz, M. Leid, The Journal of Biological Chemistry 281 (2006) 32272–32283.
[23] K. Kamimura, H. Ohi, T. Kubota, K. Okazuka, Y. Yoshikai, Y. Wakabayashi, Y. Aoyagi, Y. Mishima, R. Kominami, Biochemical and Biophysical Research Communications 355 (2007) 538–542.
[24] H. Ohi, Y. Mishima, K. Kamimura, M. Maruyama, K. Sasai, R. Kominami, Oncogene 26 (2007) 5280–5289.
[25] S. Nagel, M. Kaufmann, H.G. Drexler, R.A. MacLeod, Cancer Research 63 (2003) 5329–5334.
[26] G.K. Przybylski, W.A. Dik, J. Wanzeck, P. Grabarczyk, S. Majunke, J.I. Martin-Subero, R. Siebert, G. Dölken, W.D. Ludwig, B. Verhaaf, J.J. van Dongen, C.A. Schmidt, A.W. Langerak, Leukemia 19 (2005) 201–208.
[27] K. De Keersmaecker, P.J. Real, G.D. Gatta, T. Palomero, M.L. Sulis, V. Tosello, P. Van Vlierberghe, K. Barnes, M. Castillo, X. Sole, M. Hadler, J. Lenz, P.D. Aplan, M. Kelliher, B.L. Kee, P.P. Pandolfi, D. Kappes, F. Gounari, H. Petrie, J. Van der Meulen, F. Speleman, E. Paietta, J. Racevskis, P.H. Wiernik, J.M. Rowe, J. Soulier, D. Avran, H. Cavé, N. Dastugue, S. Raimondi, J.P. Meijerink, C. Cordon-Cardo, A. Califano, A.A. Ferrando, Nature Medicine 11 (2010) 11231–12327.
[28] A. Gutierrez, A. Kentsis, T. Sanda, L. Holmfeldt, S.C. Chen, J. Zhang, A. Protopopov, L. Chin, S.E. Dahlberg, D.S. Neuberg, L.B. Silverman, S.S. Winter, S.P. Hunger, S.E. Sallan, S. Zha, F.W. Alt, J.R. Downing, C.G. Mullighan, A.T. Look, Blood 118 (2011) 4169–4173.
[29] K. Kamimura, Y. Mishima, M. Obata, T. Endo, Y. Aoyagi, R. Kominami, Oncogene 26 (2007) 5840–5850.
[30] G.L. Bond, W. Hu, E.E. Bond, H. Robins, S.G. Lutzker, N.C. Arva, J. Bargonetti, F. Bartel, H. Taubert, P. Wuerl, K. Onel, L. Yip, S.J. Hwang, L.C. Strong, G. Lozano, A.J. Levine, Cell 119 (2004) 591–602.
[31] S. Gray, M. Levine, Current Opinion in Cell Biology 8 (1996) 358–364.
[32] A.J. Courey, S. Jia, Genes & Development 15 (2001) 2786–2796.
[33] M.G. Rosenfeld, V.V. Lunyak, C.K. Glass, Genes & Development 20 (2006) 1405–1428.
[34] C.J. Lynch, J. Milner, Oncogene 25 (2006) 3463–3470.

Leukemia Research 36 (2012) 1035–1040

Contents lists available at SciVerse ScienceDirect

Leukemia Research

journal homepage: www.elsevier.com/locate/leukres

Impairment in differentiation and cell cycle of thymocytes by loss of a *Bcl11b* tumor suppressor allele that contributes to leukemogenesis

Rieka Go[a], Kazuyoshi Takizawa[a,b], Satoshi Hirose[a], Yoshinori Katsuragi[a], Yutaka Aoyagi[b], Yukio Mishima[a], Ryo Kominami[a,*]

[a] Department of Molecular Genetics, Graduate School of Medical and Dental Sciences, Niigata University, Niigata, Japan
[b] 3rd Department of Internal Medicine, Graduate School of Medical and Dental Sciences, Niigata University, Niigata, Japan

ARTICLE INFO

Article history:
Received 27 December 2011
Received in revised form 28 April 2012
Accepted 28 April 2012
Available online 27 May 2012

Keywords:
T-ALL
BCL11B
Type B abnormalities
Haploinsufficiency
Cell cycle of thymocytes

ABSTRACT

Genetic changes in T-ALL are classified into type A abnormalities leading to arrest at a specific stage of T-cell differentiation and type B abnormalities that target cellular processes including cell cycle regulation. Mutations and deletion of a *BCL11B* haploinsuffiecient tumor suppressor allele have been found in 10–16% of T-ALL subgroups. Analysis of *Bcl11b*$^{KO/+}$ mice revealed impaired T-cell differentiation at two different stages and attenuation of γ-ray induced cell-cycle arrest at S/G2/M phase in immature CD8 single positive cells. Hence, those phenotypes provided by loss of a *Bcl11b* allele favor that *Bcl11b* mutation belongs to type B abnormalities.

1. Introduction

T-cell acute lymphoblastic leukemia (T-ALL) is a common pediatric leukemia and an aggressive malignancy of thymocytes that accounts for about 15% of ALL cases [1,2]. Leukemic transformation of immature thymocytes is caused by a multistep pathogenesis involving numerous genetic abnormalities that drive normal T-cells into uncontrolled cell growth and clonal expansion. Despite the diversity in genetic alterations, the biological processes that are targeted seem conserved throughout all T-ALL cases and affect T-cell differentiation, T-cell receptor signaling that affects cell survival, and cell cycle. The current knowledge of oncogenic and tumor suppressive mutations in T-ALL suggests a classification of these genetic defects into type A and type B abnormalities [3]. Type A abnormalities such as *TAL/LMO* alterations are a class that delineates distinct molecular-cytogenetic T-ALL subgroups and are thought to cause arrest at a specific stage of normal T-cell differentiation. The other class is type B abnormalities including *CDKN2A/2B* and *NOTCH1* mutations that are shared by several different T-ALL subgroups, and they target cellular processes including cell cycle regulation and synergize with the type A mutations during T-cell pathogenesis.

Bcl11b (B-cell CLL/lymphoma 11b) belongs to Kruppel-like C_2H_2 type zinc finger transcription proteins, the largest family of transcription factors in eukaryotes [4–7]. Although *Bcl11b* knockout (KO) mice die shortly after birth, loss of Bcl11b function is known to lead to arrest of thymocyte differentiation at different stages, indicating many roles in T-cell development [8–13]. The *Bcl11b* gene was first identified as a tumor suppressor gene by analysis of γ-ray induced mouse thymic lymphomas [4,14], a model of T-ALL [15], and genetic changes were found in more than a half of the lymphomas [4,16,17]. Recently, mutations and deletions of the human orthologue *BCL11B* have been found in 10–16% of T-ALL [18–20], and of interest, these mutations are detected irrespective of T-ALL subgroups. Accordingly, *Bcl11b* mutation may be classified into a type B abnormality, though consequences of the mutation were not investigated.

One characteristic of *Bcl11b* is haploinsufficient in its tumor suppressive capability, one wild-type allele being insufficient for tumor suppression. This is based on that most of the thymic lymphomas developed in *Bcl11b*$^{KO/+}$ mice retained the wild-type allele although thymic lymphomas developed in wild-type mice showed loss of one *Bcl11b* allele at a high frequency [16,17]. The retention of the wild-type allele was observed in spontaneously developed thymic lymphomas in *Bcl11b*$^{KO/+}$*p53*$^{KO/+}$ mice [16], and importantly, also in T-ALLs having mutations on the *BCL11B* gene [19,20]. These indicate that only loss of one *Bcl11b* allele can affect lymphomagenesis

* Corresponding author at: Department of Molecular Genetics, Graduate School of Medical and Dental Sciences, Niigata University, Asahimachi 1-757, Niigata 951-8510, Japan. Tel.: +81 25 227 2077; fax: +81 25 227 0757.
E-mail address: rykomina@med.niigata-u.ac.jp (R. Kominami).

0145-2126/$ – see front matter © 2012 Elsevier Ltd. All rights reserved.
http://dx.doi.org/10.1016/j.leukres.2012.04.028

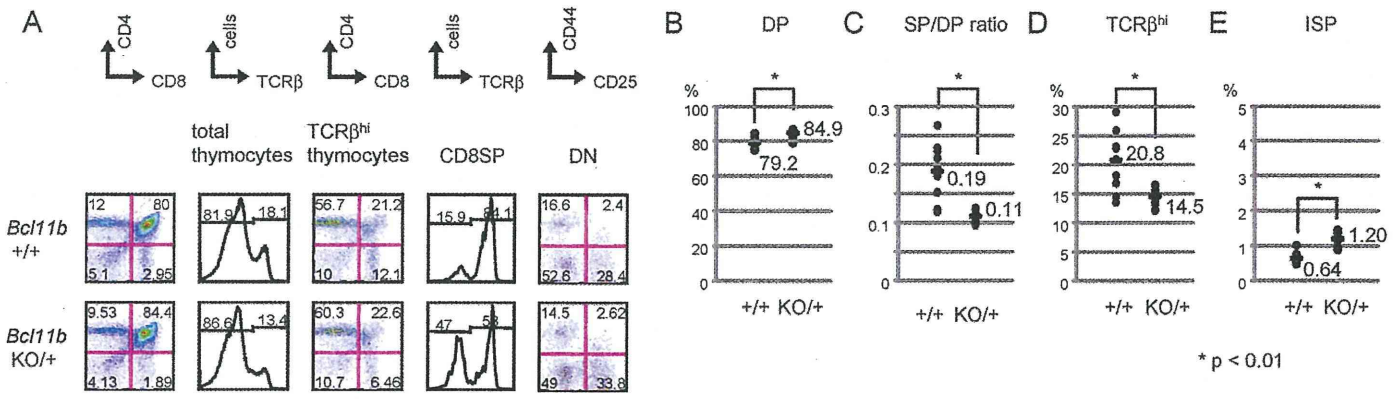

Fig. 1. Effect of *Bcl11b*$^{KO/+}$ genotype on differentiation of thymocytes. (A) Flow cytometric analysis of thymocytes from *Bcl11b*$^{+/+}$ and *Bcl11b*$^{KO/+}$ mice using CD4, CD8, TCRβ, CD25 and CD44 markers. The markers used are indicated above in each panel. As for TCRβ expression on thymocytes, total thymocytes (left) and cells in the CD4$^-$CD8$^+$ quadrant (right) were analyzed. (B, D, E) The percentage of cells and the absolute number in thymocyte subsets: B, DP cells; D, TCRβ^{high} thymocytes; E, ISP cells. (C) The ratio of SP cells/DP cells. The absolute number in average is shown below each number of the percentage. Comparison was performed between *Bcl11b*$^{+/+}$ (n = 9) and *Bcl11b*$^{KO/+}$ (n = 11) mice. *P* value for difference in the percentage between *Bcl11b*$^{+/+}$ and *Bcl11b*$^{KO/+}$ mice is less than 5% in each of B, C, D and E.

in mice and humans. Haploinsufficient capability of *Bcl11b* is also reported in tissue development [21,22]. Despite the importance of *Bcl11b* heterozygosity in lymphomagenesis, its effect on T-cell development was not studied in detail. Hence, we have examined differentiation, apoptosis, and cell cycle of thymocytes at different developmental stages in *Bcl11b*$^{KO/+}$ mice. In this paper we show that loss of a *Bcl11b* allele leads to differentiation arrest at certain immature stages and deregulation of the response to γ-radiation in cell cycle, a phenotype that may be explained by the type B alteration.

2. Materials and methods

2.1. Mice

Bcl11b$^{KO/+}$ mice were generated as described [5]. *Bcl11b*$^{+/+}$ and *Bcl11b*$^{KO/+}$ mice of the BALB/c background were subjected to γ-irradiation of 1 Gy or 3 Gy at 8 weeks of age as described [23]. Thymus or left and right thymic lobes were isolated at indicated times after irradiation and subjected to analysis. Mice used in this study were maintained under specific pathogen-free conditions in the animal colony of Niigata University. All animal experiments comply with the guidelines by the animal ethics committee for animal experimentation of the university.

2.2. Flow cytometry

Flow cytometric analysis was performed as previously described [5]. In brief, single cell suspensions of thymocytes were prepared from thymus and, 1–2 × 10^6 cells were incubated with antibodies in phosphate-buffered saline containing 2% fetal calf serum and 0.2% NaN_3 for 15 min at 4 °C. The monoclonal antibodies (mAbs) used were anti-CD4-APC or -PerCP-Cy5.5 (RM4-5 BioLegend), anti-CD8-APC or -PE (53-6.7 eBioscience), anti-CD25-FITC (PC61 BioLegend), anti-CD44-PE (IM7 Biolegend), and anti-TCRβ-FITC or -APC (H57-597 BioLegend). To prevent non-specific binding of mAbs, we added CD16/32 (93 eBioscience) before staining with labeled mAbs. Dead cells and debris were excluded from the analysis by appropriate gating of FSC and SSC. Cells were analyzed by a FACScan or a FACSCalibur (Becton-Dickinson) flow cytometer, and data were analyzed using the Flow-Jo software (Tree-Star, Inc.).

Apoptosis was measured by Annexin V assay following the manufacturer's instructions (BD Bioscience). Briefly, thymocytes were washed in cold PBS and resuspended in binding buffer (HEPES buffer supplemented with 2.5 mM $CaCl_2$). These were incubated with FITC-labeled Annexin V (BD Bioscience) for 15 min at room temperature. Flow cytometry was performed on thymocytes gated on the basis of their forward and side light scatter with any cell debris excluded from analysis. Apoptotic cells were defined as FITC$^+$ cells.

For BrdU incorporation experiments, we injected mice intra-peritoneally with 100 μl of BrdU solution (10 mg/ml). In indicated cases, irradiation was performed at 1 h after BrdU injection. Thymuses were isolated 1 h or 5 h after BrdU administration and thymocytes were fixed with cytofix/Cytoperm (BD Bioscience) and analyzed with the use of the BD Bioscience BrdU Flow Kit according to Manufacturer's instruction. In brief, cells were suspended at a concentration of 1–2 × 10^6 cells/ml, fixed, permeabilized and incubated with DNaseI (300 μg/ml) for 60 min at 37 °C. After washing, cells were incubated with FITC conjugated anti-BrdU antibodies for 20 min at room temperature. Cells were resuspended in staining buffer and analyzed by FACSCalibur flow cytometer.

Statistical analysis was done using *t*-test.

3. Results

3.1. Differentiation of thymocytes

Development of αβ T cells in the thymus proceeds through three major stages defined according to their expression pattern of CD4 and CD8 molecules on cell surface, i.e. in order of maturity, CD4$^-$CD8$^-$ double negative (DN), CD4$^+$CD8$^+$ double positive (DP), and CD4$^+$CD8$^-$ or CD4$^-$CD8$^+$ single positive cells (CD4SP or CD8SP cells, respectively) [7,24]. DP thymocytes undergo rearrangement at the TCRα locus and hence a small fraction (TCRβ^{high}-DP cells) expresses the αβ T-cell receptor (TCRαβ) complex on cell surface before progressing to TCRβ^{high}-SP stage. Immature CD8$^+$ single positive (ISP) cells exist between DN and DP stages, and they express CD8 but lack αβ TCR. DN thymocytes can be further divided into four subpopulations based on the surface expression of CD44 and CD25, with the developmental progression being CD44$^+$CD25$^-$ (DN1) to CD44$^+$CD25$^+$ (DN2) to CD44$^-$CD25$^+$ (DN3) and then to CD44$^-$CD25$^-$ (DN4) cells.

Fig. 1A shows flow cytometric analysis of thymocytes using differentiation markers that were obtained from *Bcl11b*$^{+/+}$ wild-type and *Bcl11b*$^{KO/+}$ heterozygous mice. Fig. 1B, D and E show the percentage of DP, TCRβ^{high} and ISP cells, respectively, and Supplementary Fig. 1A–D shows the absolute cell number of the thymocyte subsets. Analysis with CD4 and CD8 markers showed a higher percentage of DP cells (Fig. 1B) and a lower ratio of SP cells/DP cells (Fig. 1C) in *Bcl11b*$^{KO/+}$ thymus than in *Bcl11b*$^{+/+}$ thymus. The absolute number of DP cells was increased in *Bcl11b*$^{KO/+}$ thymus (Supplementary Fig. 1B). These results suggest developmental arrest of a certain fraction of thymocytes at DP stage in *Bcl11b*$^{KO/+}$ mice. Expression of TCRβ marker in total thymocytes showed a significantly decreased percentage of TCRβ^{high} cells in *Bcl11b*$^{KO/+}$ mice (Fig. 1D). This suggests arrest at TCRβ^{low} DP stage possibly before rearrangement at the TCRα locus.

Cells in the CD8$^+$ fraction consist of mature CD8SP cells highly expressing TCRβ and immature ISP cells with much lower expression. The percentage and the absolute number of ISP cells were higher in *Bcl11b*$^{KO/+}$ thymus than *Bcl11b*$^{+/+}$ thymus (Fig. 1E and Supplementary Fig. 1A), suggesting arrest also at the ISP stage. The CD8$^+$ fraction may include γδ T cells [10]. However, their